Region-specific and activity-dependent regulation of SVZ neurogenesis and recovery after stroke

Huixuan Liang[a], Handi Zhao[a], Amy Gleichman[a], Michal Machnicki[a], Sagar Telang[a], Sydney Tang[a], Mary Rshtouni[a], Jack Ruddell[a], and S. Thomas Carmichael[a,1]

[a]Department of Neurology, David Geffen School of Medicine, University of California, Los Angeles, CA 90095

Edited by Anders Björklund, Lund University, Lund, Sweden, and approved May 13, 2019 (received for review July 10, 2018)

Stroke is the leading cause of adult disability. Neurogenesis after stroke is associated with repair; however, the mechanisms regulating poststroke neurogenesis and its functional effect remain unclear. Here, we investigate multiple mechanistic routes of induced neurogenesis in the poststroke brain, using both a forelimb overuse manipulation that models a clinical neurorehabilitation paradigm, as well as local manipulation of cellular activity in the peri-infarct cortex. Increased activity in the forelimb peri-infarct cortex via either modulation drives increased subventricular zone (SVZ) progenitor proliferation, migration, and neuronal maturation in peri-infarct cortex. This effect is sensitive to competition from neighboring brain regions. By using orthogonal tract tracing and rabies virus approaches in transgenic SVZ-lineage-tracing mice, SVZ-derived neurons synaptically integrate into the peri-infarct cortex; these effects are enhanced with forelimb overuse. Synaptic transmission from these newborn SVZ-derived neurons is critical for spontaneous recovery after stroke, as tetanus neurotoxin silencing specifically of the SVZ-derived neurons disrupts the formation of these synaptic connections and hinders functional recovery after stroke. SVZ-derived neurogenesis after stroke is activity-dependent, region-specific, and sensitive to modulation, and the synaptic connections formed by these newborn cells are functionally critical for poststroke recovery.

neurorehabilitation | astrocyte | synapse | plasticity | motor

There is limited tissue repair and recovery after stroke. Several types of neural progenitors, arising locally in tissue around the damaged brain or migrating from the subventricular zone (SVZ), participate in a neural repair response after stroke (1–3). SVZ-derived neuronal progenitors comprise the most extensively characterized and numerically substantial poststroke neurogenic pool. Stroke induces cellular proliferation in the SVZ, migration from the SVZ to the peri-infarct tissue of immature and still-proliferating neurons (neuroblasts), and differentiation into neurons (4). A small fraction of these SVZ-derived neurons survive in the peri-infarct area (5, 6). The functional integration and role in recovery of newly derived neurons after stroke remain unclear. Experimental up-regulation of neurogenesis after stroke is associated with functional recovery (7–9), while selected ablation of adult neurogenesis early after stroke impairs recovery (10, 11). These studies have not provided definitive evidence for the synaptic integration and role of neurogenesis in recovery after stroke. There are two main conceptual limitations to studies of the role of neurogenesis in stroke. In poststroke neurogenesis, most of the newly born neurons die (12). Also, the nature of neurogenesis in adult humans is the subject of controversy (13), with conflicting studies on poststroke neurogenesis in humans (11, 14–16). One source of conflict in human poststroke neurogenesis is that recent studies dealt mostly with chronic stroke and are thus consistent with the death of most newly born, poststroke neurons in rodents. These findings point to an urgent need to identify mechanisms that may promote long-term survival in poststroke neurogenesis and that define the functional role of this process in recovery.

Activity is a key regulator of adult neurogenesis under normal physiologic conditions in both the subgranular zone and SVZ (17–20). However, how activity regulates neurogenesis after stroke is not fully understood. The major therapy for stroke recovery involves activity changes at the organismal level: Patients are put through repetitive task-specific activity in neurorehabilitation. Constraint-induced movement therapy (CIMT) is an activity-based neurorehabilitation that forces overuse of the paretic limb through restraint of the unaffected limb (21), and this recovery effect is correlated with structural plasticity (22) and functional reorganization (23). CIMT may increase proliferation of neurogenesis after stroke (24, 25). These data indicate a possible interrelationship of behavioral activity clinically in patients after stroke and behavioral or neuronal activity modulation of tissue repair through neurogenesis. However, it is unknown whether these reported effects of CIMT on neurogenesis are specific to the SVZ-derived neuroblasts; whether activity affects the specific circuits of the overused limb; and how behavioral or neuronal activity affects long-term neurogenesis and recovery.

Results

Forelimb Overuse Increases Neurogenesis in the Peri-Infarct Cortex after Stroke. Mice were forced to overuse their affected forelimb after stroke by selectively paralyzing the forelimb that was ipsilateral to the stroke (Fig. 1*A*). Focal ischemic strokes in the forelimb motor cortex were induced by photothrombosis on 2- to 4-mo-old C57BL/6 male mice (26). By using a stroke in the forelimb motor cortex, the peri-infarct cortex is within the motor cortex, including the surviving parts of the forelimb motor cortex.

Significance

Recovery after stroke involves remodeling in brain tissue adjacent to the stroke site. In this remodeling, neurogenesis after stroke involves the formation of new neurons. The role of neurogenesis in stroke recovery and the role of brain and behavioral activity in this process remain undefined. Using orthogonal transgenic mouse tracing and rabies virus approaches, we demonstrate that brain regions unexpectedly compete for new neurons after stroke and that the behavioral or cellular activity establishes this competition. These new neurons synaptically integrate into cortex, and this integration is necessary for poststroke recovery.

Author contributions: H.L. and S.T.C. designed research; H.L., H.Z., M.M., S. Telang, S. Tang, M.R., and J.R. performed research; A.G. and M.M. contributed new reagents/analytic tools; H.L., H.Z., S. Telang, and S.T.C. analyzed data; and H.L. and S.T.C. wrote the paper.

The authors declare no conflict of interest.

This article is a PNAS Direct Submission.

[1]To whom correspondence may be addressed. Email: scarmichael@mednet.ucla.edu.

This article contains supporting information online at www.pnas.org/lookup/suppl/doi:10.1073/pnas.1811825116/-/DCSupplemental.

Published online June 13, 2019.

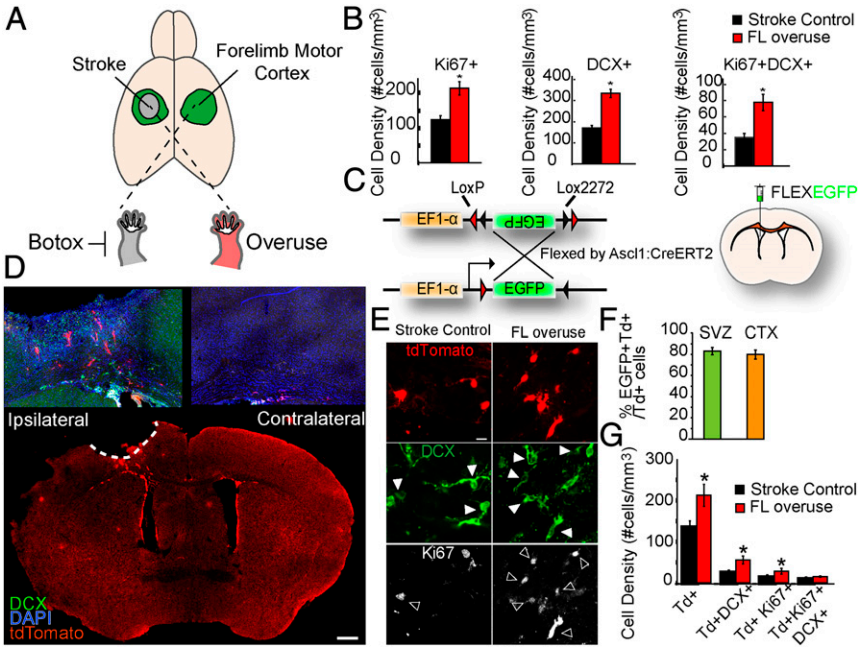

Fig. 1. Forelimb overuse increases neurogenesis in the peri-infarct cortex after stroke. (*A*) Schematic demonstration of stroke induction and forelimb overuse. Focal ischemic stroke in the forelimb motor cortex was induced by photothrombosis. To induce overuse of the paretic forelimb, Botox was injected to paralyze the nonparetic forelimb 24 h after stroke. (*B*) Density of Ki67+, DCX+, and Ki67+DCX+ cells. *$P < 0.05$. (*C*) Schematic demonstration of the EF1-α–FLEX–EGFP plasmid and lateral ventricle injection of the lentivirus expressing EF1-α–FLEX–EGFP. Lentivirus EF1-α–FLEX–EGFP was injected into the lateral ventricle of Ascl1–CreERT2::tdTomato animals 7 d before stroke. Tamoxifen was administered daily to the mice from days 2 to 7 after stroke. (*D*) Low-magnification confocal micrograph of the whole-brain coronal section with tdTomato, DCX, and DAPI 14 d after stroke. (Scale bar: 500 μm.) (*E*) Confocal micrographs of tdTomato+, DCX+, and Ki67+ cells in the peri-infarct cortex of the Ascl1–CreERT2::tdTomato mice 14 d after stroke. Filled arrowheads, tdTomato+DCX+ cells; open arrowheads, tdTomato+Ki67+ cells. (Scale bar: 5 μm.) (*F*) Percentage of EGFP+ tdTomato+ cells among total tdTomato+ cells in the SVZ and in the peri-infarct cortex 14 d after stroke. (*G*) Density of tdTomato+, tdTomato+DCX+, tdTomato+Ki67+, and tdTomato+Ki67+DCX+ cells in the peri-infarct region 14 d after stroke. *$P < 0.05$.

Mice were forced to use their paretic forelimb by administration of botulinum neurotoxin (Botox) to the unaffected forelimb 24 h after stroke to maximize the overuse behavioral activity (26). For terminology, stroke animals without Botox injection were termed stroke controls, and stroke animals with Botox injected to the nonparetic forelimb were termed FL overuse. To examine whether FL overuse affects stroke-induced neurogenesis, we first examined progenitor cell proliferation (with the marker Ki67) and neuroblast numbers (with the marker doublecortin [DCX]) in the peri-infarct cortex 14 d after stroke. Consistent with previous studies, stroke-induced neurogenesis was observed in the peri-infarct cortical region, near the stroke site, but not in the contralateral hemisphere (*SI Appendix*, Fig. S1*A*). Importantly, FL overuse enhanced neurogenesis after stroke significantly compared with the stroke control group, as demonstrated by a significantly increased density of Ki67+ progenitors (215. 20 ± 19.11 vs. 124.84 ± 11.66 cells per mm^3; $P < 0.01$), DCX+ neuroblasts (333.78 ± 19.64 vs. 170.63 ± 12.07 cells per mm^3; $P < 0.01$), and Ki67+DCX+ proliferative neuroblasts (77.87 + 10.00 vs. 34.76 ± 4.98 cells per mm^3; $P < 0.01$) in the peri-infarct cortex (Fig. 1*B* and *SI Appendix*, Fig. S1*B*). These results identify overuse of the paretic forelimb after stroke as enhancing neurogenesis in the motor cortex adjacent to the infarct and confirm a positive correlation between forced use and overall stroke-induced neurogenesis (24, 25).

Lineage Tracing of SVZ-Derived Progeny after Stroke. In addition to the SVZ, other sources of progenitors such as cortical neural progenitors (3) and parenchymal glial cells (1, 2) have been proposed to generate cortical neurons after injury. To examine the effect of forced use specifically on neurogenesis derived from the SVZ, we utilized the Ascl1–CreERT2::tdTomato transgenic animals. Ascl1 (also known as Mash1) is a basic helix–loop–helix transcription factor expressed in progenitors in the adult neurogenic niche, including the SVZ (27). The cell-specific Cre can be used for both viral (Fig. 1*C*) and germline (Fig. 1*D*) reporter labeling of SVZ-derived cells in the cortex after stroke. Consistent with previous studies, tamoxifen administration for 5 d induced a robust and specific expression of tdTomato in the Ki67+ progenitors and DCX+ neuroblasts in the SVZ and rostral migratory stream (RMS) (*SI Appendix*, Fig. S1 *C–E*). Without stroke, tdTomato+ cells were not present in nonneurogenic regions, including the cortex. In the absence of tamoxifen induction or CreERT2 expression (*SI Appendix*, Fig. S1*C*), no tdTomato expression was detected. Together, these data confirm the region- and cell-type specificity of the Ascl1–CreERT2 mice in labeling SVZ progenitors in the normal brain. Stroke induced a robust migration of TdTomato+ cells to the peri-infarct cortex by 14 d after stroke, and no such migration was observed in the contralateral hemisphere (Fig. 1*D*). Migration of TdTomato+ cells occurred gradually within the course of 14 d after stroke; the majority of cells were first found in the white matter at 3 d after stroke (*SI Appendix*, Fig. S1*G*) and then in both the white matter and peri-infarct region at 10 d after stroke (*SI Appendix*, Fig. S1*H*).

To further confirm the SVZ origin of these tdTomato cells in the peri-infarct cortex, we injected a Cre-dependent lentivirus expressing the EF1a–FLEXEGFP into the lateral ventricle of Ascl1–CreERT2 mice (Fig. 1*C* and *SI Appendix*, Fig. S2*A*). Expression of EF1a–FLEXEGFP was found at day 3 after stroke, mostly in the white matter (*SI Appendix*, Fig. S2*B*), and at days 10 (*SI Appendix*, Fig. S2*C*) and 14 in the peri-infarct region (*SI Appendix*, Fig. S2*A*). Expression of EF1a–FLEXEGFP was not found adjacent to the viral injection site in the cortex, indicating that the expression was not due to leakiness through the injection procedure (*SI Appendix*, Fig. S2*D*). In the normal brain, tamoxifen induced a coexpression of tdTomato with enhanced green fluorescent protein (EGFP) in the SVZ (Fig. 1*F* and *SI Appendix*, Fig. S2*A*), indicating induction of neural progenitors labeled through the lateral ventricle to the SVZ (EGFP) and neural progenitors through the baseline genetic cross of these mice, Ascl1–CreERT2::tdTomato. At 14 d after stroke, tdTomato+ cells from the SVZ were found in the peri-infarct motor cortex and remained highly colocalized with EGFP (Fig. 1*F* and *SI Appendix*, Fig. S2*A*). Together, these results establish the Ascl1–CreERT2::tdTomato mice as a sufficient and reliable model for lineage tracing SVZ-derived progeny after stroke.

Forelimb Overuse Increases Neurogenesis, Long-Term Survival, and Differentiation of SVZ-Derived Progeny into the Peri-Infarct Cortex. To test the effect of FL overuse on SVZ neurogenesis, stroke was induced in the Ascl1–CreERT2::tdTomato mice followed by tamoxifen induction from day 2 after stroke for 5 consecutive

days. Similar to our previous findings with labeling of all progenitors in the peri-infarct cortex (Fig. 1*B*), FL overuse for 14 d after stroke significantly increased the density of SVZ-derived tdTomato+ cells (212.39 ± 26.74 vs. 133.92 ± 16.54 cells per mm^3; $P < 0.01$), tdTomato+DCX+ neuroblasts (55.92 ± 9.63 vs. 24.59 ± 2.69 cells per mm^3; $P < 0.01$), tdTomato+Ki67+ (28.40 ± 6.62 vs. 12.59 ± 2.64 cells per mm^3; $P < 0.01$) progenitors, and numerically increased the density of tdTomato+DCX+Ki67+ (15.10 ± 3.88 vs. 8.19 ± 2.10 cells per mm^3) proliferative neuroblasts in the peri-infarct region (Fig. 1 *E* and *G*). These results demonstrate a positive effect of FL overuse in stimulating SVZ progenitor cell proliferation and SVZ-derived neuroblast migration.

Studies have demonstrated an extremely limited survival and differentiation of adult-born neurons after stroke (5, 6). We next set out to determine the long-term effect, 60 d after stroke, of FL overuse in SVZ neurogenesis and survival after stroke. Notably, FL overuse significantly induced a nearly twofold increase in tdTomato+ cell density in the peri-infarct cortex 2 mo after stroke (100.81 ± 9.18 vs. 50.80 ± 7.11 cells per mm^3; $P < 0.01$) (Fig. 2 *A* and *B*). In both the stroke control and FL overuse group, SVZ-derived tdTomato+ cells coexpressed the mature neuronal marker NeuN+ in the peri-infarct region (Fig. 2*A*); these tdTomato+ neurons coexpressed both the inhibitory neuronal marker gamma-aminobutyric acid and excitatory neuronal marker Ca/calmodulin-dependent kinase IIα (CAMKIIα) (*SI Appendix*, Fig. S3 *A* and *B*). However, the density of tdTomato+ NeuN+ mature neurons was significantly higher in the FL overuse group compared with the stroke control group (19.66 ± 2.67 vs. 5.22 ± 1.24 cells per mm^3; $P < 0.01$) (Fig. 2 *A* and *B*). Concomitantly, the percentage of NeuN+tdTomato+ among all SVZ-derived tdTomato+ cells in the FL overuse group was significantly higher than that in the stroke control group (Fig. 2*D*) (19.51 ± 2.23% vs. 10.28 ± 1.53%; $P < 0.01$). These results indicate that FL overuse after stroke increases long-term survival and maturation of neurons derived from the SVZ lineage. In addition to colabeling of an SVZ-derived marker with a mature neuronal marker in the peri-infarct cortex, in the stroke control group, a significant faction of tdTomato+ cells remained colabeled with the immature neuronal marker DCX (39.53 ± 3.44%) (Fig. 2 *C* and *D*). This fraction was significantly lower in the FL overuse condition (15.21 ± 1.97%; $P < 0.01$) (Fig. 2 *C* and *D*).

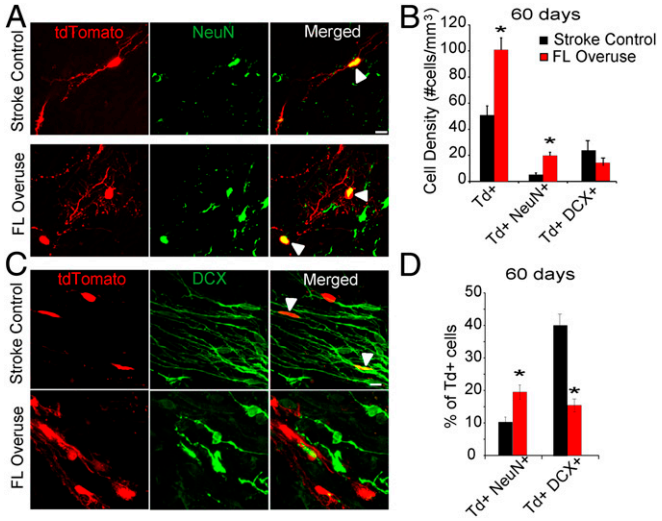

Fig. 2. Forelimb overuse increases long-term survival and neuronal differentiation of SVZ-derived progeny into the peri-infarct cortex 60 d after stroke. (*A*) Confocal micrographs of tdTomato+ and NeuN+ cells in the peri-infarct cortex of the Ascl1–CreERT2::tdTomato mice 60 d after stroke. Arrowheads, tdTomato+NeuN+ cells. (Scale bar: 5 μm.) (*B*) Quantification of density of tdTomato+, tdTomato+NeuN+, and tdTomato+DCX+ cells in the peri-infarct region. (*C*) Confocal micrographs of tdTomato+ and DCX+ cells in the peri-infarct cortex of the Ascl1–CreERT2::tdTomato mice 60 d after stroke. Arrowheads: tdTomato+DCX+ cells. (Scale bar: 5 μm.) (*D*) Percentages of tdTomato cells that coexpress NeuN and DCX in the peri-infarct region. *$P < 0.05$.

Modulation of Neuronal and Glial Activity in the Peri-Infarct Affects Poststroke Neurogenesis. These data determined that FL overuse enhances SVZ-derived cell migration to the peri-infarct motor cortex, survival, and differentiation in larger numbers compared with stroke alone. Behavioral overuse of an affected limb after stroke involves an increased excitability in the motor cortex adjacent to the stroke site (28). To directly test the role of cellular activity in neurogenesis after stroke, Designer Receptors Exclusively Activated by Designer Drugs (DREADD)-based chemogenetic tools were utilized. In addition to cortical neurons, astrocytes in the peri-infarct regions were included for modulation due to their role in regulating neuroblast migration, both in the normal and poststroke brains (29). To manipulate neuronal cell activity, lentivirus with the excitatory Gq with tdTomato was expressed under the CAMKII promotor (CAMKII-Gq). While the mechanisms by which astrocytes modulate neuronal activity are still under debate, recent evidence suggests that activation of a presumptively Gi-coupled G-protein-coupled receptor in astrocytes can inhibit neuronal activity in vivo (30). Therefore, to manipulate astrocyte activity, the inhibitory Gi with the reporter EGFP was expressed under the glial fibrillary acidic protein (GFAP) promotor (GFAP-Gi) in lentivirus. Direct measurement of immediate early gene expression indicated that these neuronal and astrocyte constructs were activated or inhibited, respectively, in each cell type (*SI Appendix*, Fig. S4 *A–D*). C57BL/6 animals were used to examined the effect of cellular activity on overall neuroblast migration, since utilization of the Ascl1–CreERT2::tdTomato animals only labels a small fraction of neuroblasts among all neuroblasts in the peri-infarct regions (14.44% in stroke control and 16.75% in FL overuse; Fig. 1 *B* and *G*), potentially due to the intrinsically low recombination efficiency of tamoxifen induction.

Lentivirus DREADD was injected into the peri-infarct cortical region 14 d before stroke to allow viral gene expression in the postinfarct period (Fig. 3 *A* and *D*). Fourteen days was chosen because the viral expression was not sufficient at days 7 and 10. Starting from 3 d after stroke, clozapine-*N*-oxide (CNO) [intraperitoneally (i.p.)] was administered twice a day for 12 consecutive days. Controls consisted of animals with DREADD viral delivery but saline administration. At 14 d after stroke, the number of DCX+ neuroblasts in the peri-infarct region was quantified in each group. To minimize variations due to the viral transfection efficiency in different animals, the ratio of DCX+/tdTomato+ and DCX+/EGFP+ was quantified. In the neuronal excitatory DREADD group, CAMKII-Gq with CNO had a significantly increased ratio of DCX+/tdTomato+ compared with saline administration (0.39 ± 0.26 vs. 0.20 ± 0.12, $P < 0.05$) (Fig. 3 *B* and *C*). Interestingly, in the astrocyte inhibitory DREADD group (GFAP-Gi), CNO induced a significantly decreased ratio of DCX+/EGFP+ compared with saline administration (0.75 ± 0.09 vs. 1.17 ± 0.10, $P < 0.05$) (Fig. 3 *E* and *F*). Note that the opposite effects of CNO in these neuronal activation and astrocyte inhibition experiments indicate that CNO by itself is not having a consistent effect outside of DREADD activation. These data show that directly stimulating the activity of excitatory neurons in the motor cortex adjacent to the stroke enhances overall neuroblast migration to the peri-infarct, whereas inhibiting astrocyte activity through DREADD-induced inhibition of astrocyte adenylate cyclase pathways reduces the amount of neuroblast migration.

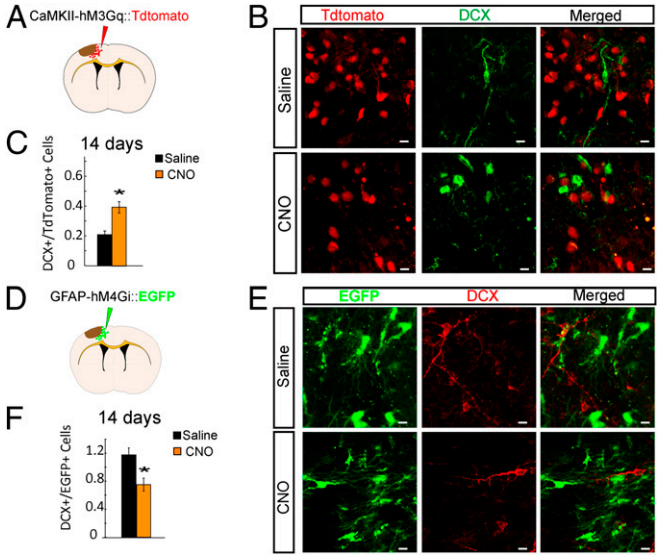

Fig. 3. Modulation of neuronal and glial activity in the peri-infarct affects poststroke neurogenesis. (*A*) Schematic of lentivirus approach with CaMKII–hM3Gq tdTomato injection. Lentivirus expressing the CaMKII–hM3Gq tdTomato was injected into the cortex 14 d before stroke. Saline or CNO was administered twice daily from day 3 until euthanizing at day 14 after stroke. (*B*) Confocal micrographs of CaMKII–hM3Gq tdTomato+ and DCX+ cells in the peri-infarct cortex, 14 d after stroke in C57BL/6 mice. (Scale bars: 5 μm.) (*C*) Ratio of numbers of DCX+ cells to numbers of tdTomato+ cells in the peri-infarct cortex. (*D*) Schematic of lentivirus approach with GFAP–hM4Gi–EGFP injection, with the same methods as in *A*. (*E*) Confocal micrographs of GFAP–hM4Gi–EGFP+ and DCX+ cells in the peri-infarct cortex, 14 d after stroke in the C57BL/6 animals. (Scale bars: 5 μm.) (*F*) Numbers of DCX+ cells to numbers of EGFP+ cells in the peri-infarct cortex. $*P < 0.05$.

Region- and Activity-Dependent Regulation on Neurogenesis after Stroke. These data identify that general behavioral activity and direct neuronal and astrocyte activity of peri-infarct motor cortex influence neurogenesis after stroke. This peri-infarct motor region is in the remaining forelimb motor cortex that is closely adjacent to the site of the forelimb motor cortex stroke and suggests a region specificity to this cellular effect: Activation of peri-infarct forelimb motor cortex enhances neurogenesis within this forelimb motor region. We next tested whether overactivity generally in cortex ipsilateral to the stroke enhances neurogenesis or whether there is a circuit specificity to this effect. Hindlimb overuse was produced through Botox injection into the hindlimb ipsilateral to the stroke, forcing overuse of the hindlimb contralateral to the stroke (the same side as was forced into overuse in the forelimb experiments above). These animals were termed HL overuse. C57BL/6 animals were used to examine the effect of HL overuse on overall neuroblast migration. The density of DCX+, Ki67+, and DCX+Ki67+ cells was significantly different among the stroke control, FL overuse, and HL overuse groups (ANOVA: $P < 0.05$). Surprisingly, with HL overuse for 14 d after stroke, there was a drastic reduction in the density of DCX+, Ki67+, and DCX+Ki67+ cells in the peri-infarct forelimb motor cortex compared with stroke control (DCX+: 66.76 ± 6.49 vs. 170.63 ± 12.07 cells per mm^3; $P < 0.01$; Ki67+: 11.71 ± 2.33 vs. 124.84 ± 11.66 cells per mm^3; $P < 0.01$; DCX+Ki67+: 8.64 ± 1.94 vs. 34.76 ± 4.98 cells per mm^3; $P < 0.05$) (Fig. 4 *A* and *B*). This result suggests that HL overuse has a surprisingly negative effect that hinders neurogenesis after stroke in another motor region. This finding raised an interesting question of whether HL overuse negatively regulates neurogenesis through modulating neuroblast migration to the forelimb peri-infarct cortex or simply diverts neuroblasts that migrate from the SVZ from the peri-infarct forelimb motor cortex into the more distant hindlimb motor cortex. Neurogenesis within the hindlimb motor cortex after stroke was studied in conditions of HL overuse, FL overuse, and stroke control. There was a significantly increased and similar number of DCX+, Ki67+, and DCX+Ki67+ cells in the hindlimb motor cortex with forced use of both FL and HL (DCX+: FL overuse 98.33 ± 13.01 vs. HL overuse 85.52 ± 14.64 cells per mm^3; $P > 0.05$; Ki67+: FL overuse 33.55 ± 9.92 vs. HL overuse 34.28 ± 8.89 cells per mm^3; $P > 0.05$; DCX+Ki67+: FL overuse 22.39 ± 7.83 vs. HL overuse 21.71 ± 6.52 cells per mm^3; $P > 0.05$) compared with stroke control (DCX+: stroke control 44.53 ± 4.46 vs. HL overuse 85.52 ± 14.64 cells per mm^3; $P < 0.05$; Ki67+: stroke control 15.13 ± 2.46 vs. HL overuse 34.28 ± 8.89 cells per mm^3; $P < 0.05$; DCX+Ki67+: stroke control 5.37 ± 1.18 vs. HL overuse 21.71 ± 6.52 cells per mm^3; $P < 0.05$) (Fig. 4 *C* and *D*). Within the HL overuse group, migration of DCX+ neuroblasts was significantly higher to the hindlimb motor cortex than to the forelimb motor cortex (HL motor cortex: 85.52 ± 14.64 vs. FL motor cortex: 66.76 ± 6.49 cells per mm^3; $P < 0.05$) (Fig. 4 *B* and *D*). Overall, these results indicate that under HL overuse, despite the overall reduction of neurogenesis in the immediately adjacent peri-infarct forelimb motor cortex, migration of neuroblasts is preferentially diverted to the more distal peri-infarct hindlimb motor cortex in which behavioral activation is performed. In summary, behavioral overactivity of forelimb motor cortex and direct neuronal overactivity in the forelimb motor cortex stimulates poststroke neurogenesis in the forelimb motor cortex, which is adjacent to the infarct, and to the more distant hindlimb motor cortex. Behavioral overactivity of the hindlimb motor cortex increases neurogenesis in the hindlimb motor cortex but, paradoxically, inhibits neurogenesis in the forelimb motor cortex.

These data imply that there is a circuit or anatomical specificity to poststroke neurogenesis, with behavioral activity in a more distant cortical site to stroke-inhibiting or outcompeting neurogenesis in a more proximal site to stroke. To further define this interaction, we tested two additional questions: Will direct neuronal activation in the hindlimb motor cortex inhibit poststroke neurogenesis in the peri-infarct forelimb motor cortex, and is there a competitive interaction between the forelimb and hindlimb motor areas in activity-dependent poststroke neurogenesis? To test these two questions, the hindlimb motor cortex was transfected with the neuronal excitatory DREADD (CAMKII-Gq) 14 d before stroke (as above) (Fig. 4 *E* and *F*), and the forelimb motor cortex was overactivated behaviorally by forcing overuse of this forelimb with Botox into the forelimb ipsilateral to the stroke. Each CAMKII-Gq DREADD transfection condition had activation with CNO and control with saline, 3–14 d after stroke. This approach created three groups: HL DREADD control, HL DREADD activation, and HL DREADD activation+FL overuse (Fig. 4*E*). HL DREADD Activation significantly decreased the density of Ki67+ and DCX+Ki67+ cells in the FL peri-infarct motor cortex, compared with the HL DREADD control ($P < 0.05$) (Fig. 4*F*). Thus, direct neuronal activation of the hindlimb motor cortex achieved either by forced behavioral use or by neuronal excitatory DREADD produced a consistent reduction of neurogenesis after stroke in the peri-infarct forelimb motor cortex. In the HL DREADD activation+FL overuse group, although the density of DCX+ cells was significantly higher than the HL DREADD control group in the FL peri-infarct motor cortex, the density of Ki67+ and DCX+Ki67+ cells was not significantly different from the HL DREADD control group (Fig. 4*F*). This result demonstrated that, unlike FL overuse alone, which up-regulates neurogenesis in peri-infarct forelimb motor cortex (Fig. 1 *B* and *G*), a combination of hindlimb neuronal activation and forelimb forced use partially diminished the effect induced by forelimb forced use alone. In summary, by using behavioral and neuronal activation,

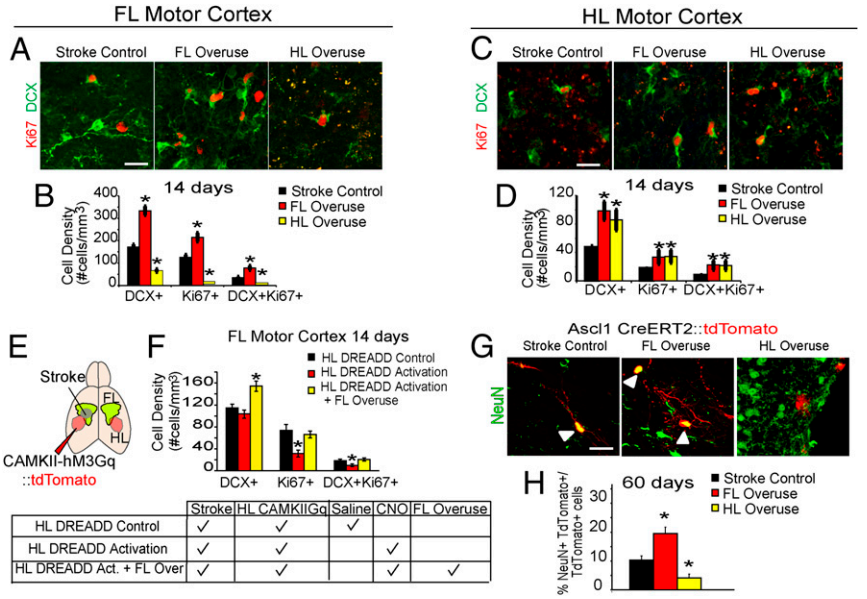

	Stroke	HL CAMKIIGq	Saline	CNO	FL Overuse
HL DREADD Control	✓	✓	✓		
HL DREADD Activation	✓	✓		✓	
HL DREADD Act. + FL Over	✓	✓		✓	✓

Fig. 4. Hindlimb overuse decreases neurogenesis in the peri-infarct forelimb motor cortex and partially offsets the neurogenic effect induced by forelimb overuse. (*A–D*) C57BL/6 stroke animals were treated with no Botox (stroke control), FL overuse, or HL overuse before euthanizing at 14 d after stroke. (*A*) Confocal micrographs of Ki67+ and DCX+ cells in the peri-infarct forelimb motor cortex. (Scale bar: 10 μm.) (*B*) Density of DCX+, Ki67+, and DCX+Ki67+ cells in the peri-infarct forelimb motor cortex. For all group comparisons, ANOVA: $P < 0.05$. (*C*) Confocal micrographs of Ki67+ and DCX+ cells in the hindlimb motor cortex. (Scale bar: 10 μm.) (*D*) Density of DCX+, Ki67+, and Ki67+DCX+ cells in the hindlimb motor cortex. For all group comparisons, ANOVA: $P < 0.05$. (*E*) Schematic of lentivirus CaMKII–hM3Gq tdTomato injection into hindlimb motor cortex. HL DREADD control group received stroke, HL CAMKII-Gq injection, and saline injection; HL DREADD activation group received stroke, HL CAMKII-Gq injection, and CNO injection; and HL DREADD activation+FL overuse group received stroke, HL CAMKII-Gq injection, CNO injection, and FL overuse. (*F*) Density of DCX+, Ki67+, and DCX+Ki67+ cells in the peri-infarct forelimb motor cortex. For all group comparisons, ANOVA: $P < 0.05$. (*G*) No Botox (stroke control), FL overuse, or HL overuse before euthanizing at 60 d after stroke in Ascl1–CreERT2::tdTomato mice. Confocal micrographs of tdTomato+ and NeuN+ in the peri-infarct forelimb motor cortex are shown. Filled arrowheads: tdTomato+ and NeuN+ mature neurons differentiated from SVZ progenitors. (Scale bar: 10 μm.) (*H*) Quantification for the percentage of percent tdTomato+ NeuN+ among all tdTomato cells in the peri-infarct region. For all group comparisons, ANOVA: $P < 0.05$. *$P < 0.05$.

these data indicate that activation of the forelimb motor cortex after stroke enhances neurogenesis in this region; activation of the hindlimb motor cortex after stroke diminishes neurogenesis in the forelimb motor cortex; and activation of the forelimb motor cortex and hindlimb motor cortex together partly offsets the effect of forelimb activation alone, producing an intermediate level of neurogenesis in the peri-infarct forelimb motor cortex. This result also indicates a counteracting effect between FL and HL cortex in regulating neurogenesis after stroke.

To further examine the long-term effect of region-specific activity regulation on neuronal differentiation in the specific cells that migrate from the SVZ, we performed HL overuse on the Ascl1–CreERT2::tdTomato mice for 2 mo after stroke. We found that, compared with stroke control and FL overuse, the percentage of tdTomato+ SVZ cells in the peri-infarct forelimb motor cortex that differentiated into NeuN+ mature neurons was significantly lower in the HL overuse group than in the stroke control group (4.10 ± 1.39 vs. 10.28 ± 1.53; $P < 0.05$; for all group comparisons, ANOVA: $P < 0.05$) (Fig. 4 *G* and *H*). This result indicates that when the more distant hindlimb motor cortex is behaviorally activated, not only neurogenesis at 14 d is reduced in the forelimb motor cortex, but the long-term neuronal differentiation of the in-migrating progenitor cells from SVZ is negatively regulated.

Forelimb Overuse Increases Synaptogenesis of SVZ-Derived Neurons in the Peri-Infarct Cortex. These data show an exquisite degree of activity-dependent regulation of the numbers and differentiation of newly born or immature neurons after stroke in the peri-infarct motor cortex. We next tested if activity also controls synaptogenesis. The expression of the presynaptic marker VGLUT1 and postsynaptic marker Homer1 was examined in the SVZ-derived tdTomato cells 2 mo after stroke (Fig. 5*A* and *SI Appendix*, Fig. S5*A*). Anterograde synaptic connections to these SVZ-derived cells in the peri-infarct motor cortex were identified by the proximity of VGlut1+ signals inside the tdTomato cells with Homer1+ signals (Fig. 5*B*) (proximity was set at a distance ≤ 0.75 μm). Similarly, retrograde synaptic formation onto the tdTomato cells from the SVZ was identified by the proximity of Homer1+ signals inside tdTomato cells with VGLUT1+ signals (Fig. 5*C*) (proximity was set at a distance ≤ 0.7 μm). Forelimb overuse induced a remarkable increase in both anterograde [FL overuse: 0.0055 ± 0.0019/tdTomato surface area (μm^2) vs. stroke control: 0.0005 ± 0.0002/tdTomato surface area (μm^2); $P < 0.01$] and retrograde synaptic connections from SVZ-derived neurons [FL overuse: 0.0039 ± 0.0016/tdTomato surface area (μm^2) vs. stroke control: 0.0006 ± 0.0002/tdTomato surface area (μm^2); $P < 0.01$], compared with SVZ-derived neurons in stroke control (Fig. 5 *B* and *C*). This result indicates that FL overuse up-regulates synaptogenesis of SVZ-derived neurons, which have migrated into the peri-infarct motor cortex.

Forelimb Overuse Increases Neural Connectivity between Peri-Infarct SVZ Neurons and Premotor Cortical Neurons. These findings of synaptic integration of SVZ neurons prompted us to determine whether this integration is involved in cortical rewiring between the peri-infarct and premotor cortex, a connection within the motor system associated with functional recovery after stroke (31–34). The Ascl1–CreERT2::tdTomato animals were used to trace neural connectivity of SVZ-derived neurons, and the neuronal tracer biotin dextran amine (BDA) was injected into the premotor cortex 7 d before euthanizing at the 2-mo post-stroke time point (Fig. 5*E*). Synaptic connections between SVZ neurons and premotor neurons were identified by proximity between BDA-filled axons to Homer1 puncta within tdTomato cells (proximity was set at a distance ≤ 0.7 μm) (Fig. 5*D*). Neurons that had migrated from the SVZ made synaptic connections with premotor axons in stroke alone within the peri-infarct motor cortex (Fig. 5 *D* and *F*). FL overuse significantly increased this number of premotor synaptic contacts, compared with the stroke control group (3.43 ± 0.25 per μm^3 vs. control stroke 2.07 ± 0.19 per μm^3, $P < 0.05$) (Fig. 5*F*). These results indicate that SVZ neurogenesis is involved in cortical rewiring with premotor cortex and forelimb forced use increasing this rewiring capacity. Moreover, unlike FL overuse, HL overuse decreased the synaptic connections between SVZ neurons and the premotor cortical neurons (0.98 ± 0.13 per μm^3 vs. control stroke 2.07 ± 0.19 per μm^3, $P < 0.05$; for all group comparison, ANOVA: $P < 0.05$) (Fig. 5*F*). Overall, these results reveal a circuit-specific and activity-dependent regulation in cortical

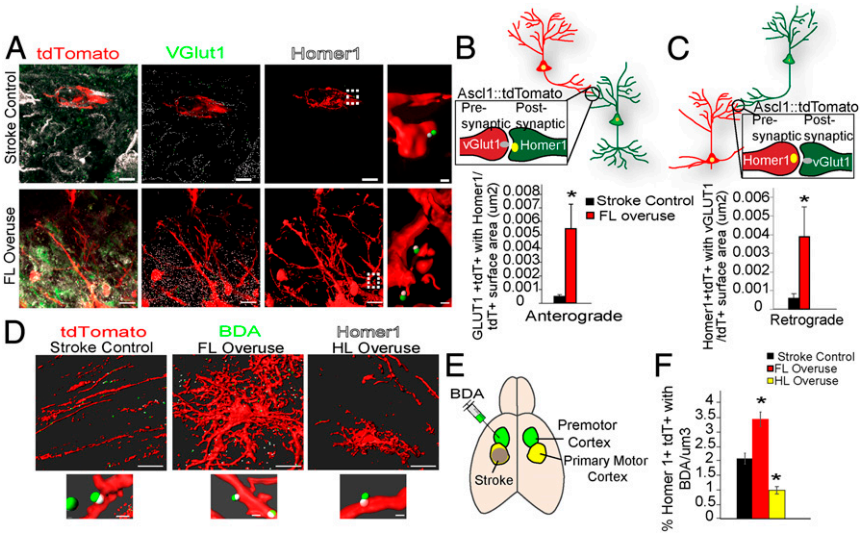

Fig. 5. Forelimb overuse increases synaptogenesis and neural connectivity from the SVZ-derived progenitors. (*A–C*) Ascl1–CreERT2(+);tdTomato animals induced with stroke and tamoxifen were treated with no Botox (control) or FL overuse before euthanizing at 60 d after stroke. (*A*) Confocal micrographs of tdTomato+ (red), VGlut1+ (green) presynaptic proteins, and Homer1+ (white) postsynaptic proteins in the peri-infarct cortex of Ascl1–CreERT2::tdTomato mice. Images are segmented (Imaris, Bitplane). (Scale bars: 10 μm.) The rightmost images show a higher magnification of colocation of VGLUT1 with the postsynaptic Homer1, from the corresponding regions highlighted with the dashed lines. (Scale bars: 2 μm.) (*B*) Anterograde synapses identified by the colocalization of tdTomato+VGLUT1+ with Homer1. Quantification is number of anterograde synaptic formations per tdTomato cell surface (μm^2). (*C*) Retrograde synapses identified by colocalization of tdTomato+Homer1+ with VGLUT1. Quantifications is the number of retrograde synaptic formation per tdTomato cell surface (μm^2). (*D–F*) BDA was injected into the premotor cortex of Ascl1–CreERT2(+);tdTomato stroke animals 7 d before euthanizing at the poststroke day-60 time point. These animals received either no Botox (stroke control), FL overuse, or HL overuse. (*D*) Segmented images (Imaris) of colocation of Homer1 within the tdTomato cells with BDA axons. (*D*, *Lower*) Higher-magnification images. [Scale bars: 10 μm (*Upper*) and 2 μm (*Lower*).] (*E*) Schematic illustration of stroke induction and BDA injection. (*F*) Number of colocalizations between tdTomato+Homer1+ and BDA+ per μm^3. For all group comparisons, ANOVA: $P < 0.05$. *$P < 0.05$.

rewiring, between the peri-infarct SVZ neurons with the premotor cortical neurons.

Forelimb Forced Use Increases Monosynaptic Connectivity of SVZ-Derived Neurons in the Peri-Infarct Cortex. To further examine the direct synaptic connectivity of SVZ-derived neurons in peri-infarct motor cortex, we next utilized a recombinant rabies virus (RABV) approach. RABV identifies direct synaptic connections through monosynaptic retrograde transfection (35–37). To achieve cell-type-specific tracing of SVZ-derived neurons, we utilized a Cre-dependent targeting approach combined with RABV (38). In short, the Cre-dependent adeno-associated virus (AAV) FLEXBTG virus expressing the reporter GFP, tumor virus A receptor, and glycoprotein G was injected into the lateral ventricle of the Ascl1–CreERT2::tdTomato animals (*SI Appendix*, Fig. S6*A*). This provides neural progenitors in the SVZ with a receptor for the RABV and part of the machinery for virus production. The rest of the RABV construct was injected only into the peri-infarct motor cortex, so that transsynaptic labeling could only occur with neurons that migrated from the SVZ to the peri-infarct motor cortex. Stroke was induced 7 d after AAV FLEXBTG injection into the ventricle, followed by tamoxifen induction for 5 consecutive days. Animals were allowed to survive for 2 mo after stroke, and the RABV expressing blue fluorescent protein (BFP) was then injected into the peri-infarct regions 4 d before euthanizing (*SI Appendix*, Fig. S6*A*). By using this approach, progenitors in the SVZ were initially targeted by the AAV FLEXBTG and expressed both GFP and tdTomato upon tamoxifen induction. These progenitors with subsequent migration to the peri-infarct and viral targeting by RABV BFP were termed starter cells, expressing tdTomato, GFP, and BFP (Fig. 6*B* and *SI Appendix*, Fig. S6*B*). Cells with retrograde monosynaptic connections with starter cells were termed connected cells, expressing BFP only (*SI Appendix*, Fig. S6*B*). This viral-targeting approach is both sufficient and specific to the SVZ lineage, as shown by a high percentage of colabeling with tdTomato and GFP in the SVZ and cortex from the nonstroke mice (*SI Appendix*, Fig. S6 *A* and *B*). BFP-only cells, indicating a monosynaptic connection to SVZ-derived neurons, were readily detected with injection of RABV into the peri-infarct region done at a time point 2 mo after stroke (Fig. 6*B*). This approach is specific: In this cortical-injection approach, BFP cells were not detected in the olfactory bulb, indicating that there was no general neurogenesis synaptic labeling, and there was no synaptic labeling in the cortex from animals receiving only AAV FLEXBTG, but not RABV, injection.

To quantify synaptic strength, we employed the input connection strength index (CSI) (39). CSI refers to the ratio of connected cell numbers vs. the starter cell numbers and thus is a marker of connection number and not the strength of a synaptic connection. BFP-only cells were present both in the stroke control and FL overuse groups (Fig. 6*B*), providing evidence for a monosynaptic connection from SVZ neurons after stroke. Additionally, BFP-only cells were found to be both tdTomato+ or tdTomato−, and sparse BFP+ cells were found in the contralateral cortex (*SI Appendix*, Fig. S7 *A–C*). Importantly, FL overuse significantly increased CSI compared with the stroke control group (stroke control: 1.02 ± 0.04 vs. FL overuse: 3.53 ± 0.57; $P < 0.05$) (Fig. 6*C*). This result indicates that FL overuse increases SVZ-derived neuronal synaptic connections in the motor cortex after stroke.

To gain a more comprehensive understanding of this connective strength, we compared the CSI of SVZ-derived neurons to that of the normal cortical neurons resident in this region of the motor cortex. To target cortical neurons, AAV Synapsin–Cre was coinjected with AAV FLEXBTG in the cortical area corresponding to the same peri-infarct region described in the previous experiment (*SI Appendix*, Fig. S6*A*). At 7 d after

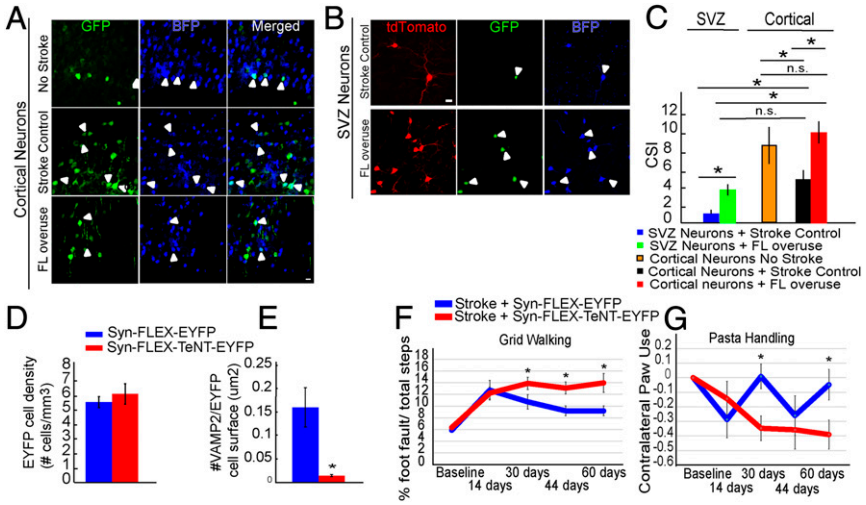

Fig. 6. Forelimb overuse increases the monosynaptic neural connectivity of SVZ-derived neurons, and synaptic connectivity is required for functional recovery. (*A*) AAV Synapsin-Cre and AAV FLEXBTG were co-injected into the peri-infarct cortex 7 d before stroke. Animals were allowed to survive 2 months after stroke and the rabies BFP was injected into the same region 4 d before sacrifice. Arrowheads show GFP+BFP+ starter cells. (Scale bar: 5 μm.) (*B*) Confocal micrographs of tdTomato+, GFP+ and BFP+ SVZ-derived neurons forming monosynaptic connections in the peri-infarct. Arrowheads show GFP+BFP+ starter cells. (Scale bar: 5 μm.) (*C*) Quantification of synaptic connection with the cortical strength index from either cortical neurons or SVZ-derived neurons. $*P <$ 0.05. n.s., not significant. (*D*) EYFP cell density in the peri-infarct regions 2 mo after stroke. (*E*) Quantification for the number of VAMP2 located within EYFP+ cells per EYFP cell surface. (*F*) Quantification for percentage of foot faults from the total number of steps, based on the grid-walk task. (*G*) Quantification of (right paw duration − left paw duration)/total duration, based on the pasta-handling task. $*P < 0.05$.

injection, animals were given a stroke (control animals had no stroke) and then survived for 2 mo. RABV was injected in the peri-infarct 4 d before euthanizing. Without stroke, we found a strong input connection from cortical neurons, as demonstrated by a high CSI (8.06 ± 1.92) (Fig. 6 *A* and *C*). This CSI represented a baseline connection strength under this experiment regiment in normal (nonstroke) motor cortical neurons. Stroke decreased the CSI of cortical neurons in the stroke control compared with the nonstroke level (cortical neurons stroke control: 4.59 ± 0.97 vs. cortical neurons no stroke: 8.06 ± 1.92; $P < 0.05$) (Fig. 6 *A* and *C*). In the FL overuse after stroke, the CSI of cortical neurons was significantly higher than the stroke control (9.48 ± 1.15 vs. 4.59 ± 0.97; $P < 0.05$) (Fig. 6 *A* and *C*). The CSI of cortical neurons under FL overuse reached a comparable level to that of cortical neurons without stroke ($P > 0.05$) (Fig. 6 *A* and *C*). These results indicated that the input connectivity strength of cortical neurons significantly decreases after stroke and that forced use largely compensates this loss of connection strength. Further, even though SVZ neurons integrate into the circuit of peri-infarct motor cortex, their input connection did not reach the same strength as the preexisting cortical neurons surviving after stroke. Interestingly, under FL overuse, the connection strength of SVZ neurons reached a comparable level with the preexisting cortical neurons from the stroke control group (Fig. 6 *A*–*C*). This result suggests that forced use enhances the potential of neural connectivity of SVZ neurons, which might be otherwise intrinsically limited under the nonactivity-enhanced stroke.

Circuit Formation from SVZ Neurons Is Involved in Motor Functional Recovery after Stroke. To directly address whether this synaptic integration is relevant to functional recovery after stroke, we next employed tetanus toxin (TeNT) to silence SVZ-derived neurons. TeNT silences neurons by inhibiting vesicular transmitter release, and TeNT-mediated neuronal silencing has been utilized to dissect the function of distinct neural circuits (40). This approach avoids the possible inflammatory stimulus that occurs with cell ablation approaches. We utilized a Cre-dependent AAV FLEX virus expressing TeNT and GFP under the synapsin promotor (hSyn-FLEX-TeNT-GFP) (*SI Appendix*, Fig. S6*C*). AAV-hSyn-FLEX-GFP expressing only GFP was used as the control virus (*SI Appendix*, Fig. S6*C*). To specifically target SVZ-derived neurons, AAV hSyn-FLEX-TeNT-GFP or the control AAV-hSyn-FLEX-GFP was coinjected with AAV cytomegalovirus–Cre into the lateral ventricle 7 d before stroke (*SI Appendix*, Fig. S6*C*). Behavior analyses, including grid-walking and pasta-handling, were performed to assess forelimb motor function recovery after stroke (26). In the control and TeNT groups, enhanced yellow fluorescent protein-positive (EYFP+) cells were apparent in the peri-infarct regions 2 mo after stroke, and the density of EYFP+ cells was insignificantly different between these two groups (control: 55.67 ± 3.79 vs. TeNT: 61.62 ± 7.10 cells per mm^3; $P > 0.05$) (Fig. 6*D* and *SI Appendix*, Fig. S6*D*). Vesicle-associated membrane protein 2 (VAMP2) expression was significantly decreased in the TeNT EYFP+ cells [control: 0.16 ± 0.05 vs. TeNT: 0.01 ± 0.002 #VAMP2+EYFP+/EYFP cell surface (μm^2); $P < 0.01$] (*SI Appendix*, Fig. S6*E* and Fig. 6*E*), confirming the sufficient synaptic disruption mediated by TeNT. Stroke produces an impairment in forelimb motor control, as seen in deterioration in the grid-walking and pasta-handling tasks, with some recovery toward baseline over 2 mo (Fig. 6 *F* and *G*). When SVZ-derived neuronal progenitor cells express TeNT, this recovery is blocked. In the grid-walking behavior task, the TeNT group displayed a significantly higher percentage of foot faults starting from 30 d after stroke (control vs. TeNT, 30 d: 10.73 ± 1.24% vs. 13.90 ± 1.05%; 45 d: 9.20 ± 0.86% vs. 13.08 ± 1.02%; 60 d: 9.18 ± 0.82% vs. 13.98 ± 1.61%; all timepoints with $P < 0.05$). (Fig. 6*F*). Notably, with TeNT, these behavior impairments persisted for up to 2 mo after stroke, a timepoint when partial spontaneous recovery was achieved in the stroke control virus group (Fig. 6*F*). Similarly, stroke with TeNT produced a significant decrease in pasta-handling using the paretic forelimb at 30 d after stroke (control vs. TeNT, 0.01 ± 0.08 vs. −0.35 ± 0.08; $P < 0.05$) (Fig. 6*G*). The failure to recover motor impairment in the TeNT groups was present at 2 mo, when the stroke control groups performed at the level of baseline,

indicating spontaneous recovery (control vs. TeNT: -0.05 ± 0.11 vs. -0.39 ± 0.10; $P < 0.05$) (Fig. 6*G*). These behavioral results suggest that disruption of synaptic formation specifically of SVZ-derived neurons prevents some degree of recovery after stroke.

Discussion

Stroke induces SVZ-derived neuroblasts to migrate to the regions around the infarct and differentiate into neurons (5, 41). Despite a limited survival rate, these newborn neurons display morphological features, molecular marker expression, electrophysiological properties, and gene-expression profiles that correspond to mature neurons (5, 42–44). However, whether these neurons are functional and relevant to stroke recovery remains largely unknown. Our study identifies three principles in poststroke neurogenesis. Heightened activity of peri-infarct cortex through behavioral or direct neuronal activation induces poststroke neurogenesis by enhancing proliferation, migration, maturation, and circuit integration of SVZ-derived immature neurons. Heightened activity of cortical areas more distant to the infarct than the peri-infarct cortex can divert these migrating neuroblasts into that brain region from their usual migration target and blunt the effects of heightened activation of the peri-infarct cortex. Synaptic function from SVZ-derived neurons after stroke is essential to functional recovery.

Synaptic Integration of SVZ-Derived Neurons after Stroke. Synaptic integration of the SVZ-derived neurons was rigorously determined by using three independent approaches, including synaptic marker examination, BDA neuroanatomical labeling of cortico-cortical connections, and RABV-based monosynaptic tracing. Expression of both the presynaptic marker VGLUT1 and the postsynaptic marker Homer1 detected within the SVZ-derived neurons indicated that these cells possess the molecular machinery required for neurotransmission, aligned in the appropriate presynaptic and postsynaptic orientation. The existence of local connections was supported by RABV-based monosynaptic tracing of direct connections from neighboring neurons in the peri-infarct cortex to SVZ-derived neurons in the local circuitry of the motor cortex adjacent to stroke.

In addition to local connections, we also identified long-distance cortico-cortical connections involving neurons from the premotor cortex to SVZ-derived neurons in the motor cortex, based on labeling of the connections with the tracer BDA. Axonal sprouting in premotor connections or an enhanced role of motor–premotor connections has been extensively reported in stroke and is linked to functional recovery (26, 31–33). Our study confirms this finding and provides evidence of involvement of SVZ-derived neurons in such a connection. Whether the SVZ-derived neurons are connected to other brain regions reported to interact with the peri-infarct motor cortex remains to be determined.

Synaptic Integration through Forelimb Activity. Previous studies have shown that overuse of the paretic limb, mimicking CIMT, up-regulates neurogenesis after stroke (24, 25). However, the scope of these studies has been mainly focused on the proliferation of neural progenitors in the SVZ and the survival of overall newborn neurons in the peri-infarct cortex. Whether long-term neuronal maturation and synaptic integration of these neurons is influenced by behavioral overuse or direct neuronal activation is unknown. Our findings provide strong evidence demonstrating that limb overuse increases synaptic integration of SVZ-derived neurons, from three methods for experimental definition for synaptogenesis. First, synaptic marker analysis revealed a profound increase of SVZ-derived synaptogenesis after forelimb forced use, both in anterograde and retrograde synaptic formations. Second, forced use increases synaptic contacts between SVZ-derived neurons with premotor cortical neurons. Third, monosynaptic tracing revealed a significant increase of direct presynaptic connections to SVZ neurons after forelimb forced use. These data reveal an activity- or experience-dependent synaptic plasticity on SVZ neurons. It remains to be determined whether this plasticity takes place during the initial establishment of synaptic connections or during a possible fine-tuning stage when modification or pruning may occur on existing synapses.

A relevant conceptual framework may come from the role of activity in the regulation of synaptic plasticity of adult-born granule cells (abGCs) in the olfactory bulb, a neuronal population that originates from the same progenitor pools in the SVZ. Soon after arrival in the olfactory bulb, abGCs begin to respond to odor and stay responsive during the first 3 wk of arrival (45). This time frame corresponds closely with the critical period for synaptogenesis, during which synaptic formation in abGCs is particularly sensitive to olfactory exposure (46, 47). In our study, forelimb forced use was initiated 2 d after stroke, before the period when SVZ-derived neuroblasts are estimated to arrive at the peri-infarct cortex (8). Therefore, it is likely that the stimuli driven by forelimb forced use affects SVZ-derived neurons from the early stage of synaptogenesis and synaptic integration inside the peri-infarct region. The question as to what extent synaptogenesis of these neurons remains sensitive to behavioral stimuli or neuronal activity levels and whether a prolonged stimulus is required to maintain its regulatory effect is unclear. Moreover, it is unclear whether SVZ-derived neurons have the same critical period as described for their siblings that migrate to the olfactory bulb.

Functional Significance of Synaptic Integration of SVZ-Derived Neurons. Neurogenesis in the human brain has been the subject of some controversy. There is evidence for and against active neurogenesis in the human subgranular zone and SVZ (48–50) and discussion of the limited techniques available for the determination of neurogenesis in humans (13). One technique using ^{14}C dating has shown robust neurogenesis in the human SVZ and contribution of adult neurons to the basal ganglia in the normal brain (50) and no neurogenesis after cortical stroke (12). These data are mostly from chronic stroke and support the finding in rodents that most newly born neurons in the adult brain after stroke eventually die. Other studies, using different methodologies, have identified immature neurons and poststroke neurogenesis after stroke in humans (14–16). The present studies address this problem of limited long-term neurogenesis after stroke with attention to activity-dependent mechanisms to enhance this process.

There has been limited evidence for an association of poststroke neurogenesis with recovery. Systematic delivery of pro-neurogenesis factors such as fibroblast growth factor 2, stromal-derived factor 1, and angiopoietin 1 improve functional recovery after stroke (7–9). However, many growth factors associated with stroke recovery also increase angiogenesis or axonal sprouting, processes that are associated with poststroke functional recovery (8). Ablation of adult-born neurons before stroke induction, by using genetic approaches with thymidine kinase expression and ganciclovir treatment, impedes recovery (51). Ablation of all neural precursor cells, including both the SVZ and hippocampal neuroblasts, cause hippocampal-dependent deficits after stroke (51). However, these hippocampal deficits may potentially interfere with the behavioral tasks that assess function of neuroblasts that migrate to areas of damage after stroke. Moreover, treatments depleting neuroblasts or neural progenitors before stroke could cause adverse effects on neuroprotection rather than effects on hindering recovery. To overcome these limitations, we established a technique that allows us to manipulate neuronal function specifically associated with the SVZ-derived neuronal lineage.

Stroke in the forelimb motor cortex produces impaired motor function in gait and in spontaneous forelimb exploration, with a recovery toward prestroke (normal) motor control. However, blocking vesicular release in SVZ-derived neurons with selective expression of TeNT prevents this motor recovery. This vesicular release blockade did not cause cell death due to TeNT expression, because the SVZ-derived neuronal cell density in the peri-infarct cortex between control and TeNT groups was insignificantly different. This result is consistent with previous studies in which expression of TeNT does not cause neuronal cell death (52). Our results demonstrate a specific requirement of proper synaptic function from SVZ-derived neurons in stroke recovery. Future experiments will be required to determine whether a gain of synaptic function in this population enhances stroke recovery.

Synaptic inhibition mediated by TeNT not only affects the synaptic integration which happens at later stages, but potentially interferes with neuronal maturation, which occurs from an earlier stage. This maturation interference could occur because the immature neurons with TeNT cannot experience neuronal activity, which is critical for neuronal maturation. In addition, a nonsynaptic interaction of the SVZ-derived neurons with the peri-infarct tissue could be important, as suggested. This nonsynaptic interaction might be through local growth factor or other molecule release. However, the fact that we did not observe any significant behavioral recovery changes between TeNT and the control group until 30 d after stroke indicates that the immature neuron recovery effect is not very likely due to events that are simply the result of having an immature neuron in the midst of damaged cortex. The prorecovery effect of these SVZ-derived neurons occurs after a month-long process within the peri-infarct tissue, and this is the time period of maturation and synaptic connection of the in-migrating immature neurons.

Region-Specific Effect of Activity Regulation. Two regions were targeted for activity modulations in this study: the forelimb motor cortex immediately adjacent to the infarct and the hindlimb motor cortex that is more distant but connected to the infarct. These two areas were either behaviorally activated through administration of Botox to the ipsilateral musculature or pharmacogenetically activated through neuronal stimulation or astrocytic inhibition with DREADD. While behavior interactions at the interhemispheric level have been examined, little is known about intrahemispheric interactions. The ipsilateral hindlimb motor cortex, as part of the peri-infarct region further away from the infarct boundary than the forelimb motor cortex, was examined in this study. There is anatomical and functional overlap between the forelimb and hindlimb motor representations in the rodent (53, 54). Moreover, following large strokes to the forelimb motor cortex, hindlimb corticospinal neurons may assume forelimb function, potentially through connections with surviving forelimb neurons (55). Perhaps the most surprising finding from our study is that behavioral and direct neuronal activation in the forelimb motor cortex vs. the hindlimb motor cortex have counteracting effects in poststroke neurogenesis; forelimb overuse up-regulates neurogenesis in both the near (forelimb) and more distant (hindlimb) peri-infarct cortex, while hindlimb overuse down-regulates migrating neuroblasts to the peri-infarct forelimb motor cortex. This inhibitory effect exerted from hindlimb overuse may derive from several sources. Activity in the hindlimb cortex diverted migration of neuroblasts from the peri-infarct forelimb motor cortex to the more distant (to the SVZ origin) hindlimb motor cortex. Hindlimb overuse might also impact neuronal activity and hence survival of SVZ-derived neuroblasts in the peri-infarct forelimb motor cortex—more cells might die in the peri-infarct forelimb motor cortex when the hindlimb motor cortex is overactive. These interactions of activity-dependent effects on neurogenesis by different cortical areas and their connections has implications for the patterned behavioral activity induced in neurorehabilitation. In these clinical activities, arm use is enhanced through repetitive task-specific activities and, in clinical trials, robotic repetition of arm use (56, 57). If a degree of spontaneous biological recovery involves poststroke neurogenesis, as indicated in this study, and this neurogenesis is exquisitely sensitive to cortical activity patterns, neurorehabilitation interventions in humans should be directly impacting the cellular biology of the brain.

Methods

Animals. Animal procedures were performed in accordance with the National Institutes of Health Animal Protection Guidelines and the University of California Los Angeles Chancellor's Animal Research Committee. We used 2- to 4-mo-old male C57BL/6 [Jackson Laboratories (Jackson Lab)] mice. Ascl1–CreERT2 [Ascl1tm1.1(Cre/ERT2) Jejo; Jackson Lab, catalog no. 012882] were crossed to the Cre-dependent reporter mice expressing tdTomato [B6; 129S6 Gt(ROSA)26Sortm14(CAG-tdTomato)Hze; Jackson Lab, catalog number 007908]. Tamoxifen at 48 h was administered (100 mg/kg i.p. per day for 5 d).

Photothrombotic Ischemia and Forced Use. Forelimb motor cortex stroke was induced by photothrombosis as described (26). Body temperature was maintained at 37.0 °C with a heating pad throughout the procedure. A total of 0.15 μL of Botox diluted to a concentration of 1:8 was injected into five forelimb muscle compartments 24 h after stroke, with 0.03 μL administered intramuscularly at each site. Control animals with stroke received vehicle.

Tissue Processing and Immunohistochemistry. Mice were euthanized, and tissue was processed for immunohistochemical staining as described (8, 26). Primary antibodies used in this study included goat DCX (Santa Cruz Biotechnology, catalog no. C-18), rabbit Ki67 (Abcam, catalog no. ab15580), GFP Tag Polyclonal Antibody (Invitrogen, catalog no. A-11122), mouse NeuN (Millipore, catalog no. MAB377), guinea pig VGLUT1 (Millipore, catalog no. AB5905), rabbit Homer 1 (Synaptic Systems, catalog no. 160003), rabbit phosphor-ERK (Cell Signaling Technology, catalog no. 4370p), rabbit Zif268 (Cell Signaling Technology, catalog no. 4154), and rat VAMP2 (Abcam, catalog no. ab181754).

DREADD. A total of 2 μL of lentivirus CaMKIIa–hM3D(Gq) –tdTomato or GFAP–hM4D(Gi)–P2A–lckGFP-miR124T was delivered via intracerebral injections [anterior/posterior (A/P): 0 mm, medial/lateral (M/L): –0.75 mm, dorsal/ventral (D/V): 0.5 mm] 14 d before stroke. Astrocytic expression was driven by the minimal human GFAP promoter (58), and specificity was enhanced through the addition of an miR124 targeting sequence (58). CNO (Enzo Life Sciences) was i.p. administered beginning 3 d after stroke (1 mg/kg, twice a day, 12 consecutive days). Control animals received saline injection.

Rabies Monosynaptic Tracing and Analysis. AAV2-EF1a-FLEX-BTG (Salk Institute Gene Transfer Targeting and Therapeutics Core) at a volume of 5 μL was delivered via the lateral ventricle (A/P: 0 mm, M/L: –0.75 mm, D/V: 1.7 mm). Stroke was induced in the Ascl1–CreERT2::tdTomato animals 7 d after injection, and tamoxifen was administered (100 mg/kg, 5 d). After 2 mo, 4 d before euthanizing, EnvA G-deleted rabies BFP (Salk Institute Gene Transfer Targeting and Therapeutics Core) was injected at a volume of 2 μL into two sites of the peri-infarct region (no. 1, A/P: 0 mm, M/L: –0.75 mm, D/V: 0.5 mm; and no. 2, A/P: 0 mm, M/L: –1.5 mm, D/V: 0.7 mm). AAV9-Synapsin–Cre (SignaGen Laboratories) and AAV2-EF1a-FLEX-BTG were mixed at a ratio of 1:1, and 2 μL of the viral mixture was delivered via intracerebral injection (A/P: 0 mm, M/L: 0.75 mm, D/V: 0.5 mm) 7 d before stroke. Stroke induction, tamoxifen administration, and EnvA G-deleted rabies BFP were performed as described above. AAV9–Synapsin–Cre (SignaGen Laboratories) and AAV2–EF1a–FLEX–BTG were mixed at a ratio of 1:1, and 2 μL of the viral mixture was delivered via intracerebral injection (A/P: 0 mm, M/L: –0.75 mm, D/V: 0.5 mm). Animals received no stroke and were allowed to survive for 2 mo. EnvA G-deleted rabies BFP was injected under the same condition as described. The input CSI was used as described (39). All sections with the peri-infarct regions were selected for analysis, and the total numbers of the GFP+BFP+ cells (starter cells) and GFP–BFP+ cells (monosynaptic connected cells) were counted in the peri-infarct cortex. CSI was then calculated based on CSI = (numbers of GFP–BFP+ cells)/(numbers of GFP+BFP+ cells).

Viral Packaging and Behavioral Assessment after Stroke. The plasmids pAAV-hSyn-Flex-GFP and pAAV-hSyn-Flex-TeNT-P2A-GFP were a gift from Fan Wang, Departments of Neurobiology and Cell Biology, Duke University Medical Center, Durham, NC. Mice ($n = 15$ per group) were tested on the grid-walking and pasta-handling tests as described (26). For the grid-walk test, stroke deficit was calculated by percent (number of right foot faults/total number of steps). For the

pasta-handling task, deficit was calculated by (duration of the right paw pasta holding − duration of the left paw pasta holding)/total duration of pasta holding. This number from each animal at different poststroke timepoints was subtracted by the number calculated for the same animal at baseline, to normalize the paw preference for individual animals.

Synapse Analysis. Axon surface rendering was applied to generate the surface of tdTomato cells (Imaris, Bitplane). VGLUT1 and Homer1 were detected by using the Spot detection function in this system. Identification of synaptic markers located inside the tdTomato cells was achieved by first creating a mask channel for the tdTomato cell surface, followed by spot detection within the masked channel. The spot colocalization distance was set at 0.75 μm, which corresponded to the average sum of the radius from the VGLUT1 and Homer1 puncta. To normalize the number of colocalized synapse per cell surface, the number of colocalized spots was divided by the surface area of tdTomato cells.

BDA Labeling. At 2 mo after stroke, 0.4 μL of 10% BDA (wt/vol; Sigma) was injected into the premotor cortex (A/P:1.8 mm, M/L: −1.75 mm, D/V: 0.75 mm). BDA was visualized by treatment with streptavidin–Alexa Fluor 594.

Data Analysis. Significance was determined by using Student's *t* test or one-way ANOVA (for multiple group analysis). When ANOVA was used for statistical analysis, it is clarified in *Results* or the figure legends. All values were expressed as mean + SEM. $*P < 0.05$, $n = 8$ per group. All data were analyzed blinded to condition. Mice were randomized into the experimental group.

1. B. Bi *et al*., Cortical glial fibrillary acidic protein-positive cells generate neurons after perinatal hypoxic injury. *J. Neurosci.* **31**, 9205–9221 (2011a).
2. A. Buffo *et al*., Origin and progeny of reactive gliosis: A source of multipotent cells in the injured brain. *Proc. Natl. Acad. Sci. U.S.A.* **105**, 3581–3586 (2008).
3. K. Ohira *et al*., Ischemia-induced neurogenesis of neocortical layer 1 progenitor cells. *Nat. Neurosci.* **13**, 173–179 (2010).
4. V. Donega, O. Raineteau, Postnatal neural stem cells: Probing their competence for cortical repair. *Neuroscientist* **23**, 605–615 (2017).
5. A. Arvidsson, T. Collin, D. Kirik, Z. Kokaia, O. Lindvall, Neuronal replacement from endogenous precursors in the adult brain after stroke. *Nat. Med.* **8**, 963–970 (2002).
6. P. Thored *et al*., Persistent production of neurons from adult brain stem cells during recovery after stroke. *Stem Cells* **24**, 739–747 (2006).
7. R. R. Leker *et al*., Long-lasting regeneration after ischemia in the cerebral cortex. *Stroke* **38**, 153–161 (2007).
8. J. J. Ohab, S. Fleming, A. Blesch, S. T. Carmichael, A neurovascular niche for neurogenesis after stroke. *J. Neurosci.* **26**, 13007–13016 (2006).
9. L. Wang, Z. Zhang, Y. Wang, R. Zhang, M. Chopp, Treatment of stroke with erythropoietin enhances neurogenesis and angiogenesis and improves neurological function in rats. *Stroke* **35**, 1732–1737 (2004).
10. A. D. R. Garcia, N. B. Doan, T. Imura, T. G. Bush, M. V. Sofroniew, GFAP-expressing progenitors are the principal source of constitutive neurogenesis in adult mouse forebrain. *Nat. Neurosci.* **7**, 1233–1241 (2004).
11. I. Imayoshi *et al*., Roles of continuous neurogenesis in the structural and functional integrity of the adult forebrain. *Nat. Neurosci.* **11**, 1153–1161 (2008).
12. H. B. Huttner *et al*., The age and genomic integrity of neurons after cortical stroke in humans. *Nat. Neurosci.* **17**, 801–803 (2014).
13. H. Lee, S. Thuret, Adult human hippocampal neurogenesis: Controversy and evidence. *Trends Mol. Med.* **24**, 521–522 (2018).
14. K. Jin *et al*., Evidence for stroke-induced neurogenesis in the human brain. *Proc. Natl. Acad. Sci. U.S.A.* **103**, 13198–13202 (2006).
15. J. Macas, C. Nern, K. H. Plate, S. Momma, Increased generation of neuronal progenitors after ischemic injury in the aged adult human forebrain. *J. Neurosci.* **26**, 13114–13119 (2006).
16. J. Martí-Fàbregas *et al*., Proliferation in the human ipsilateral subventricular zone after ischemic stroke. *Neurology* **74**, 357–365 (2010).
17. G. Kempermann, Activity dependency and aging in the regulation of adult neurogenesis. *Cold Spring Harb. Perspect. Biol.* **7**, a018929 (2015).
18. C. Rochefort, G. Gheusi, J.-D. Vincent, P.-M. Lledo, Enriched odor exposure increases the number of newborn neurons in the adult olfactory bulb and improves odor memory. *J. Neurosci.* **22**, 2679–2689 (2002).
19. H. van Praag, G. Kempermann, F. H. Gage, Running increases cell proliferation and neurogenesis in the adult mouse dentate gyrus. *Nat. Neurosci.* **2**, 266–270 (1999).
20. S.-M. Ra *et al*., Treadmill running and swimming increase cell proliferation in the hippocampal dentate gyrus of rats. *Neurosci. Lett.* **333**, 123–126 (2002).
21. G. Kwakkel, J. M. Veerbeek, E. E. H. van Wegen, S. L. Wolf, Constraint-induced movement therapy after stroke. *Lancet Neurol.* **14**, 224–234 (2015).
22. L. V. Gauthier *et al*., Remodeling the brain: Plastic structural brain changes produced by different motor therapies after stroke. *Stroke* **39**, 1520–1525 (2008).
23. M. Könönen *et al*., Functional MRI and motor behavioral changes obtained with constraint-induced movement therapy in chronic stroke. *Eur. J. Neurol.* **19**, 578–586 (2012).
24. C. Zhao, J. Wang, S. Zhao, Y. Nie, Constraint-induced movement therapy enhanced neurogenesis and behavioral recovery after stroke in adult rats. *Tohoku J. Exp. Med.* **218**, 301–308 (2009).
25. H. L. Qu *et al*., Forced limb-use enhanced neurogenesis and behavioral recovery after stroke in the aged rats. *Neuroscience* **286**, 316–324 (2015).
26. J. J. Overman *et al*., A role for ephrin-A5 in axonal sprouting, recovery, and activity-dependent plasticity after stroke. *Proc. Natl. Acad. Sci. U.S.A.* **109**, E2230–E2239 (2012).
27. E. J. Kim, J. L. Ables, L. K. Dickel, A. J. Eisch, J. E. Johnson, Ascl1 (Mash1) defines cells with long-term neurogenic potential in subgranular and subventricular zones in adult mouse brain. *PLoS One* **6**, e18472 (2011).
28. M. Lucas *et al*., Neurorestorative effects of constraint-induced movement therapy after stroke: An integrative review. *Neurosci. Med.* **4**, 253–262 (2013).
29. A. Gengatharan, R. R. Bammann, A. Saghatelyan, The role of astrocytes in the generation, migration, and integration of new neurons in the adult olfactory bulb. *Front. Neurosci.* **10**, 149 (2016).
30. Z. Ma, T. Stork, D. E. Bergles, M. R. Freeman, Neuromodulators signal through astrocytes to alter neural circuit activity and behaviour. *Nature* **539**, 428–432 (2016).
31. N. Dancause *et al*., Extensive cortical rewiring after brain injury. *J. Neurosci.* **25**, 10167–10179 (2005).
32. S. S. Kantak, J. W. Stinear, E. R. Buch, L. G. Cohen, Rewiring the brain: Potential role of the premotor cortex in motor control, learning, and recovery of function following brain injury. *Neurorehabil. Neural Repair* **26**, 282–292 (2012).
33. S. R. Zeiler, J. W. Krakauer, The interaction between training and plasticity in the poststroke brain. *Curr. Opin. Neurol.* **26**, 609–616 (2013).
34. S. R. Zeiler *et al*., Medial premotor cortex shows a reduction in inhibitory markers and mediates recovery in a mouse model of focal stroke. *Stroke* **44**, 483–489 (2013).
35. E. M. Callaway, Transneuronal circuit tracing with neurotropic viruses. *Curr. Opin. Neurobiol.* **18**, 617–623 (2008).
36. J. H. Marshel, T. Mori, K. J. Nielsen, E. M. Callaway, Targeting single neuronal networks for gene expression and cell labeling in vivo. *Neuron* **67**, 562–574 (2010).
37. I. R. Wickersham *et al*., Monosynaptic restriction of transsynaptic tracing from single, genetically targeted neurons. *Neuron* **53**, 639–647 (2007).
38. N. R. Wall, I. R. Wickersham, A. Cetin, M. De La Parra, E. M. Callaway, Monosynaptic circuit tracing in vivo through Cre-dependent targeting and complementation of modified rabies virus. *Proc. Natl. Acad. Sci. U.S.A.* **107**, 21848–21853 (2010).
39. Y. Sun *et al*., Cell-type-specific circuit connectivity of hippocampal CA1 revealed through Cre-dependent rabies tracing. *Cell Rep.* **7**, 269–280 (2014).
40. C. R. Yu *et al*., Spontaneous neural activity is required for the establishment and maintenance of the olfactory sensory map. *Neuron* **42**, 553–566 (2004).
41. M. Kreuzberg *et al*., Increased subventricular zone-derived cortical neurogenesis after ischemic lesion. *Exp. Neurol.* **226**, 90–99 (2010).
42. B. Lai, X. O. Mao, L. Xie, K. Jin, D. A. Greenberg, Electrophysiological neurodifferentiation of subventricular zone-derived precursor cells following stroke. *Neurosci. Lett.* **442**, 305–308 (2008).
43. X. S. Liu *et al*., Stroke induces gene profile changes associated with neurogenesis and angiogenesis in adult subventricular zone progenitor cells. *J. Cereb. Blood Flow Metab.* **27**, 564–574 (2007).
44. T. Yamashita *et al*., Subventricular zone-derived neuroblasts migrate and differentiate into mature neurons in the post-stroke adult striatum. *J. Neurosci.* **26**, 6627–6636 (2006).
45. J. L. Wallace, M. Wienisch, V. N. Murthy, Development and refinement of functional properties of adult-born neurons. *Neuron* **96**, 883–896.e7 (2017).
46. W. Kelsch, C.-W. Lin, C. P. Mosley, C. Lois, A critical period for activity-dependent synaptic development during olfactory bulb adult neurogenesis. *J. Neurosci.* **29**, 11852–11858 (2009).
47. A. Saghatelyan *et al*., Activity-dependent adjustments of the inhibitory network in the olfactory bulb following early postnatal deprivation. *Neuron* **46**, 103–116 (2005).
48. M. Boldrini *et al*., Human hippocampal neurogenesis persists throughout aging. *Cell Stem Cell* **22**, 589–599.e5 (2018).
49. S. F. Sorrells *et al*., Human hippocampal neurogenesis drops sharply in children to undetectable levels in adults. *Nature* **555**, 377–381 (2018).
50. A. Ernst *et al*., Neurogenesis in the striatum of the adult human brain. *Cell* **156**, 1072–1083 (2014).
51. C. Sun *et al*., Conditional ablation of neuroprogenitor cells in adult mice impedes recovery of poststroke cognitive function and reduces synaptic connectivity in the perforant pathway. *J. Neurosci.* **33**, 17314–17325 (2013).
52. E. Foster *et al*., Targeted ablation, silencing, and activation establish glycinergic dorsal horn neurons as key components of a spinal gate for pain and itch. *Neuron* **85**, 1289–1304 (2015).
53. K. A. Tennant *et al*., The organization of the forelimb representation of the C57BL/6 mouse motor cortex as defined by intracortical microstimulation and cytoarchitecture. *Cereb. Cortex* **21**, 865–876 (2011).
54. O. G. S. Ayling, T. C. Harrison, J. D. Boyd, A. Goroshkov, T. H. Murphy, Automated light-based mapping of motor cortex by photoactivation of channelrhodopsin-2 transgenic mice. *Nat. Methods* **6**, 219–224 (2009).
55. M. L. Starkey *et al*., Back seat driving: Hindlimb corticospinal neurons assume forelimb control following ischaemic stroke. *Brain* **135**, 3265–3281 (2012).
56. A. C. Lo *et al*., Robot-assisted therapy for long-term upper-limb impairment after stroke. *N. Engl. J. Med.* **362**, 1772–1783 (2010).
57. C. E. Lang *et al*., Dose response of task-specific upper limb training in people at least 6 months poststroke: A phase II, single-blind, randomized, controlled trial. *Ann. Neurol.* **80**, 342–354 (2016).
58. Y. Lee, A. Messing, M. Su, M. Brenner, GFAP promoter elements required for region-specific and astrocyte-specific expression. *Glia* **56**, 481–493 (2008).